Pharmacokinetics of *dl*-praeruptorin A after single-dose intravenous administration to rats with liver cirrhosis

Zhang Z, Liang XF, Su MQ, Yang Q, Li LP, Zhang XH, Wang XM, *Zhu X

School of Pharmaceutical Science, Xiamen University, Xiamen, China

ABSTRACT

Background and the purpose of the study: As a novel drug in the treatment of cardiac diseases, *dl*-praeruptorin A (Pd-Ia) is the major active component of traditional herbal medicine *Peucedanum praeruptorum* Dunn and is metabolized primarily via cytochrome P450 isozymes (CYP) 3A1 and 3A2 in rats. In the present study, the influence of liver cirrhosis on pharmacokinetics of Pd-Ia and hepatic mRNA expression of CYP3A1 and 3A2 in rats with experimental liver cirrhosis (LC rats) were evaluated.

Methods: Pd-Ia was given intravenously (5 mg·kg^{-1}) to LC rats induced by dimethylnitrosamine and pharmacokinetic variables were measured. Enzyme kinetic metabolism of Pd-Ia in rat hepatic microsomes was also investigated and hepatic mRNA expression of CYP3A1 and 3A2 were measured by real-time PCR.

Results and major conclusion: After intravenous administration in LC rats, the area under the plasma concentration-time curve from time zero to infinity ($AUC_{0-\infty}$) was significantly greater than that in control rats, which might be due to slower rate of the hepatic blood flow and significant slower hepatic intrinsic clearance (CL_{int}) in rats. The decreased metabolic clearance of Pd-Ia in LC rats might be at least partly caused by the decreased levels of CYP3A1 and 3A2 responsible for Pd-Ia metabolism. These findings may provide new insights into the inter- and intra-individual pharmacokinetic variability of Pd-Ia.

Keywords: Pd-Ia, rats, Dimethylnitrosamine, Pharmacokinetic alteration.

INTRODUCTION

dl-Praeruptorin A (Pd-Ia, Fig 1) is the major active component of traditional herbal medicine *Peucedanum praeruptorum* Dunn and has been proved to be a novel Ca^{2+} influx blocker (1). It has been reported that Pd-Ia could inhibit the expression of apoptosis related proteins, reduce the level of proinflammatory factors, and increase intermediate filament desmin and vimentin contents in ischemia/ reperfusion myocardiocytes (2-4). Additionally, Pd-Ia has been reported to be an effective therapeutic drug for treatment of the contractile defects associated with cardiac hypertrophy (5). Therefore, Pd-Ia has drawn increasing attentions and displayed bright prospects in prevention and therapy of cardiac diseases.

The pharmacokinetics, tissue distribution and excretion of Pd-Ia in rats following a single intravenous (i.v.) administration have been investigated by our group. Few intact form of Pd-Ia was excreted by bile and kidney, which might be resulted from liver first pass effects (6). Moreover, based on in vitro study, liver could be the main metabolizing organ and Pd-Ia is primarily metabolized via hepatic cytochrome P450 isozymes

(CYP) 3A1 and 3A2 in rats (not reported). The aim of this study was to investigate the influence of liver cirrhosis on the pharmacokinetics of Pd-Ia after i.v. administration (5 mg·kg^{-1}) to rats induced by dimethylnitrosamine.

Drug metabolism by CYP isozymes has important clinical consequences because of the possibility of reduced drug metabolism and subsequent increased plasma drug concentrations in subjects with liver dysfunctions (7). Liver cirrhosis is a chronic disease with high mortality rate. An experimental liver cirrhotic rat model induced by dimethylnitrosamine was used in this study, which simulates the clinical features of human liver cirrhosis such as mortality, ascites, hepatic parenchymal cell destruction, formation of connective tissue and nodular regeneration (8). It has also been reported that dimethylnitrosamine-induced liver cirrhosis in rats is reproducible (9).

MATERIALS AND METHODS

Materials

Pd-Ia (purity > 98 %) was kindly donated by Prof. Okuyama T (Meiji College of Pharmacy, Tokyo, Japan). Diazepam (purity > 98 %, internal

standard), dimethylnitrosamine and Tris®-buffer were obtained from Sigma-Aldrich (MO, USA). Reduced form of β-nicotinamide adenine dinucleotide phosphate (NADPH) was purchased from Roche (Basel, Switzerland). Detection kits for total proteins, albumin, glutamate oxaloacetate transaminase (GOT), glutamate pyruvate transaminase (GPT), total bilirubin and direct bilirubin were obtained from Nanjing Jiancheng Bioengineering Institute (Nanjing, China). Other chemicals were of analytical or HPLC grades.

Induction of liver cirrhosis
Male Sprague-Dawley rats (4–5 weeks old, 180–200 g) were randomly divided into liver cirrhosis (LC) and control groups. Freshly prepared dimethylnitrosamine (solution in physiological saline) at a dose of 0.01 mg·kg^{-1} was injected intraperitoneally to LC rats on three consecutive days of the week for 4 weeks (10). For control rats, the same volume of physiological saline was injected. Experiments were carried out seven days after the last dimethylnitrosamine injection or physiological saline.

Preliminary study and real-time PCR analysis of CYP3A1 and 3A2
The serum of control and LC rats (n=5, respectively) were collected for the measurement of total protein, albumin, GOT, GPT, total bilirubin and direct bilirubin. The whole kidney, spleen, and liver of each rat were excised, rinsed with physiological saline, blotted dry and weighed (10).
Hepatic total RNA was extracted using the TRIzol extraction method (Sigma-Aldrich, USA) according to the manufacturer's instructions. Reverse transcription of extracted total RNA to cDNA was performed using a reverse transcription kit (TaKaRa, Japan). Then, the SYBR Green real-time PCR amplification and detection were performed using the ABI 7500 System (Applied Biosystems, USA) and the selective primers for CYP3A1 (sense primer: 5'-GAGGCCCAGCTAGAGGGACAACA-3', antisense primer: 5'-CGTAGAGGAGCACCAGGACGACT-3') (125 bp), CYP3A2 (sense primer: 5'-GGATTCTAA GCATAAGCACCGAGTG-3', antisense primer: 5'-GGCCAGGAAATACAAGACAAAGGA G-3') (187 bp), and β-actin (sense primer: 5'-CCCTGTGCTGCTCACCGA-3', antisense primer: 5'-ACAGTGTGGGTGACCCCGTC-3') (170 bp) genes. The cDNA amplifications were carried out in a 20 µl reaction volume containing 10 µl of Power SYBR® Green master mix, 0.5 µl each of forward and reverse primers (10 µmol·l^{-1}), 4 µl of cDNA and 5 µl of purified water. Thermal profile for real-time PCR was 95 °C for 10 min, and 45 cycles at

95 °C for 15 sec and 60 °C for 1 min, followed by the melting curve. The target mRNA levels ($n = 4$ for both groups) were normalized with the β-actin mRNA level.

Enzyme kinetic metabolism of Pd-Ia
Rat hepatic microsomes were prepared and the protein content was measured by the reported methods (11, 12). Microsomal fractions (equivalent to 0.5 mg of protein) were mixed with 50 µl of 0.1 mol·l^{-1} Tris®-buffer, pH 7.4, containing 1 mmol·l^{-1} NADPH; 5 µl of Pd-Ia (solutions in dimethylsulfoxide at concentrations of 5, 10, 25, 50, 100, 250 and 500 µmol·l^{-1}) and 0.1 mol·l^{-1} Tris®-buffer, sufficient to a final volume of 0.5 ml. The reaction mixtures were incubated in a water-bath shaker at 37 °C for 3 min, and then terminated by placing them on ice. All above incubation conditions were linear and Pd-Ia was measured by LC-MS/MS (13). The kinetic parameters (K_m, V_{max}) for the disappearance of Pd-Ia were calculated using the nonlinear regression method (14). The intrinsic clearance (CL_{int}) for the disappearance of Pd-Ia per milligram of protein was calculated by dividing the V_{max} by the K_m.

Pharmacokinetic study of Pd-Ia
The cannulation of the jugular vein and carotid artery was performed for the pretreatment of rats (15). Pd-Ia (solution in PEG400 / Tween80 / physiological saline 1:1:8, v/v/v) at a dose of 5 mg·kg^{-1} was infused via the jugular vein to rats in both groups (n=8, respectively). Following administration of Pd-Ia, a blood sample (approximately 0.2 ml) was collected via the carotid artery at 0 (control), 1 (at the end of the infusion), 5, 15, 30, 60, 90, 120, 180, 240, 360 and 480 min. Each blood sample was immediately centrifuged and a 100 µl of supernatant plasma layer was transferred into another tube and stored at -80 °C until analysis. The 8 hrs bile was collected via bile duct cannulation for each rat in both groups. At the end of the experiment (24 hrs), each metabolic cage was rinsed with 10 ml of distilled water and the rinsings were combined with 24 hrs urine. Then each rat was sacrificed and the entire gastrointestinal tract was removed and homogenated. Concentrations of Pd-Ia in the above samples were measured by LC-MS/MS (13) and pharmacokinetic parameters were calculated using WinNonlin Professional Edition Version 2.1 (Pharsight Corporation, USA).

RESULTS AND DISCUSSION
Body weight, organ weight and serum biochemical data in control and LC rats are listed in table 1. Body weight gain decreased significantly in LC rats (from 192 to 274 g) compared with that in control rats (from 189 to 372 g). In LC rats, the whole liver and kidney weight were lower (55.1% and 17.9% decrease, respectively), but the whole spleen weight

Table 1. Mean (± SD) body weight, organ weight and serum biochemical data in control and LC rats ($n = 5$, respectively).

Parameters	Control	Liver Cirrhosis
Initial body weight (g)	189±14.4	192±11.5
Final body weight (g)	372±28.2	274±25.6 **
Liver weight (g)	13.8±1.9	6.2±1.5 **
Liver weight (% of body weight)	3.7±0.53	2.2±0.36 **
Kidney weight (g)	2.8±0.29	2.1±0.27 **
Kidney weight (% of body weight)	0.75±0.062	0.79±0.092 *
Spleen weight (g)	0.85±0.077	1.3±0.29 **
Spleen weight (% of body weight)	0.23±0.029	0.47±0.095 **
Serum		
Total proteins (g·dl^{-1})	6.46±0.60	4.01±0.45 **
Albumin (g·dl^{-1})	3.41±0.49	2.27±0.44 **
GOT (IU·l^{-1})	99.5±16.3	183.6±21.6 **
GPT (IU·l^{-1})	45.4±9.8	102.5±22.5 **
Total bilirubin (mg·dl^{-1})	0.29±0.023	1.13±0.15 **
Direct bilirubin (mg·dl^{-1})	0.046±0.0095	0.252±0.0554 **

$^{*}P < 0.05$, $^{**}P < 0.01$, significant difference compared to control

Table 2. Mean (± SD) kinetic parameters for the disappearance of Pd-Ia in control and LC rats ($n = 6$, respectively).

Parameters	Control	Liver Cirrhosis
V_{max} (nmol·min^{-1}·mg protein^{-1})	59.5±2.8	21.7±2.6 **
K_{m} (µmol·l^{-1})	238±31.6	233±27.9
CL_{int} (ml·min^{-1}·mg protein^{-1})	0.25±0.049	0.093±0.0094 **

V_{max}: maximum velocity; K_{m}: Michaelis-Menten constant; CL_{int}: intrinsic clearance
$^{**}P < 0.01$, significant difference compared to control

was significantly higher (52.4% increase) than those in control rats. The liver weight based on percentage of body weight was significantly lower (39.9% decrease), however, the kidney and spleen weight based on percentage of body weight was higher (11.9% and 107.0% increase, respectively) in LC rats. Compared with the control rats, the LC rats had significant decrease in serum levels of total protein (37.9%) and albumin (33.4%); significant increased serum levels of GOT (84.5% increase), GPT (125.7% increase), total bilirubin (289.7%) and direct bilirubin (447.8%). The data suggested that the presence of liver cirrhosis in LC rats was apparent.

Cirrhosis may alter drug disposition by a variety of mechanisms including a reduction in absolute cell mass with function retained in surviving cells; changes in the enzyme levels and/or activity in surviving hepatocytes; impaired drug entry into hepatocytes; and impaired uptake of oxygen (16). To further evaluate the potential mechanisms responsible for the metabolism of Pd-Ia in LC rats, changes in the hepatic mRNA expression of CYP3A1 and 3A2 were investigated and are shown in figure 2. The hepatic mRNA expression of CYP3A1 and 3A2 in

LC rats decreased significantly (73.1% and 64.1%, respectively), compared with that of control rats.

Table 2 shows that the maximum velocity (V_{max}) for the disappearance of Pd-Ia in LC rats was significantly slower (63.4% decrease) than that of control rats, suggesting that the maximal ability to metabolize Pd-Ia in hepatic microsomes was significantly slower. However, the Michaelis-Menten constant (K_{m}) was not significantly different between two groups suggesting that the affinity of Pd-Ia to the enzyme(s) was not changed in LC rats. Hence, the intrinsic clearance (CL_{int}) for the disappearance of Pd-Ia in LC rats was significantly slower (62.8% decrease) than that of control rats suggesting that metabolism of Pd-Ia could be slower in LC rats.
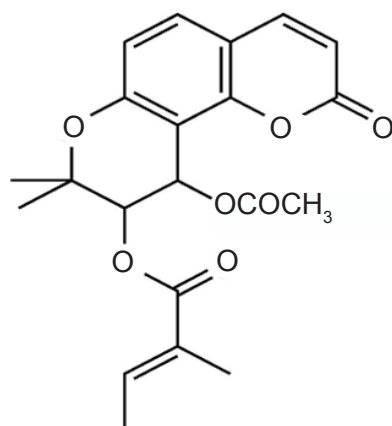
The mean arterial plasma concentration-time curves of Pd-Ia after i.v. administration at a single dose of 5 mg·kg^{-1} to control and LC rats are shown in figure 3, and the relevant pharmacokinetic parameters are listed in table 3. After i.v. administration, the mean arterial plasma concentrations of Pd-Ia were higher in LC rats, and this resulted in a significant greater AUC$_{0-\infty}$ (63.5% increase). The terminal half-life ($t_{1/2}$) in LC rats was significantly longer (67.9% increase) and the total body clearance (CL) was significantly lower

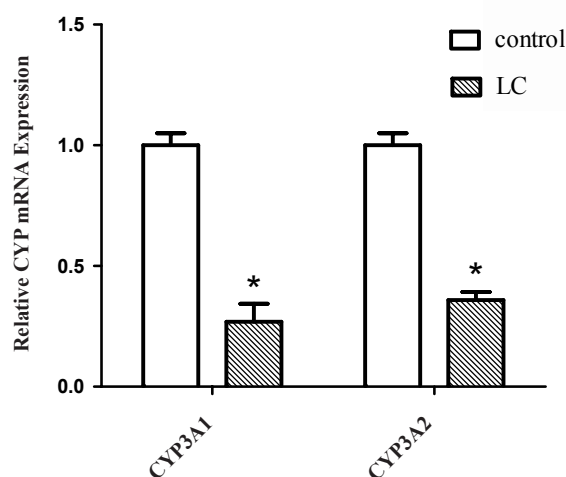**Table 3.** Mean (± SD) pharmacokinetic parameters of Pd-Ia after intravenous administration

Parameters	Control	Liver Cirrhosis
Initial body weight (g)	190±13.4	189±12.5
Final body weight (g)	376±21.6	269±18.6 **
$AUC_{0-\infty}$ (min·µg·ml^{-1})	68.4±13.9	111.8±29.7 **
$t_{1/2}$ (min)	59.2±9.0	99.4±10.8 **
CL (ml·min^{-1})	15.5±2.3	8.3±1.8 **
V_z (l)	1.3±0.26	1.2±0.35
8 h Bile (% of dose)	0.092±0.0033	0.126±0.0060 **
$Ae_{0-24\,h}$ (% of dose)	0.114±0.0166	0.156±0.0252 **
$GI_{24\,h}$ (% of dose)	BDL	BDL

$AUC_{0-\infty}$: area under the analyte concentrations versus time curve from time 0 to infinity; $t_{1/2}$: terminal half-life; CL: **total body clearance;** V_z: terminal volume of distribution; $Ae_{0-24\,h}$: urine samples at 24 hrs; $GI_{24\,h}$: gastrointestinal tract samples at 24 hrs
BDL: below the detection limit.
**$P < 0.01$, significant difference compared to control.

Figure 1. The chemical structure of **Pd-Ia**.

Figure 2. Hepatic mRNA expression of CYP3A1 and CYP3A2 in **control and LC rats was measured by real-time PCR. Open and** hatched columns indicate relative mRNA levels. Each column and bar represents mean ± SD for 6 experiments. *$P < 0.05$, significant difference compared to control.

(46.4% decrease). The total amount of unchanged Pd-Ia excreted in 24 hrs urine ($Ae_{0-24\,h}$, expressed in terms of percentage of i.v. dose) were 0.114% and 0.156% for control and LC rats, respectively. These results indicated that the contribution of renal clearance (CL_R) to CL of Pd-Ia was almost negligible and the CL of Pd-Ia could represent nonrenal clearance (CL_{NR}) in rats. Moreover, unchanged Pd-Ia recovered from the gastrointestinal tract at 24 hrs ($GI_{24\,h}$) was below detection limit for both groups; the total amount of unchanged Pd-Ia in 8 hrs bile (expressed in terms of percentage of i.v. dose) were 0.092% and 0.126% for control and LC rats, suggesting that the contribution of gastrointestinal and biliary excretion to CL_{NR} of Pd-Ia was also negligible. Hence, the CL_{NR} could represent hepatic intrinsic clearance (CL_{int}) of Pd-Ia which was metabolized almost completely after i.v. administration.

The $AUC_{0-\infty}$ after *i.v.* administration of **Pd-Ia in LC** rats was significantly higher than that in control rats, possibly as a result of the significant slower CL of Pd-Ia (Table 3). Since the CL_{NR} of Pd-Ia could represent its metabolic clearance and **Pd-Ia was metabolized** almost completely after i.v. administration in rats, the slower CL could be due to significant slower hepatic CL_{int} for the disappearance of Pd-Ia (Table 2) and slower hepatic blood flow rate (17). The slower hepatic CL_{int} could be at least partly attributed to significant decrease in mRNA expression of CYP3A1 and 3A2 compared with that in control rats (Fig 2) since Pd-Ia is primarily metabolized via hepatic CYP3A1 and 3A2 in rats. Moreover, it has been reported that the protein expression of hepatic
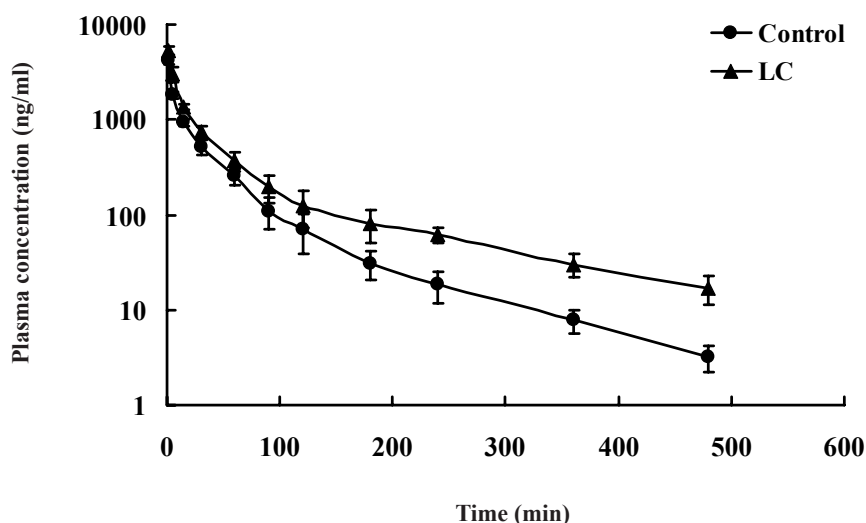
Figure 3. Mean (± SD) plasma concentration-time curves of Pd-Ia after intravenous administration at a dose of 5 mg·kg^{-1} to control rats (●; *n*=8) and LC rats (▲; *n*=8).

CYP3A was decreased in LC rats (18).

CONCLUSION

The present results suggest that after i.v. administration of Pd-Ia at a single dose of 5 mg·kg^{-1} to LC rats, the AUC$_{0-\infty}$ was significantly greater than that of the control rats which could be due to slower hepatic blood flow rate and significant slower hepatic CL$_{int}$ in rats. In addition, the decreased metabolic clearance of Pd-Ia in LC rats might be at least partly caused by the decreased levels of CYP3A1 and 3A2 responsible for Pd-Ia metabolism. These findings may provide new insights into the inter- and intra-individual pharmacokinetic variability of Pd-Ia.

REFERENCES

1. Kozawa T, Sakai K, Uchida M, Okuyama T, Shibata S. Calcium antagonistic action of a coumarin isolated from "Qian-Hu", a Chinese traditional medicine. J. Pharm. Pharmacol, 1981; 33: 317-320.
2. Chang TH, Liu XY, Zhang XH, Wang HL. Effects of *dl*-praeruptorin A on interleukin-6 level and Fas, bax, bcl-2 protein expression in ischemia-reperfusion myocardium. Acta Pharmacol. Sin, 2002; 23: 769-774.
3. Wang C, Chang TH, Zhang XH, Wang HL. Effects of *dl*-praeruptorin A on nucleus factor-κB and tumor necrosis factor-α expression in ischemia reperfusion hearts. Acta Pharmacol. Sin, 2004; 25: 35-40.
4. Chang H, Chu XY, Zou J, Chang TH. Effect of *dl*-praeruptorin A on desmin and vimentin content in rat ischemia/reperfusion myocardiocytes. Chin. Med. J, 2007; 120: 2256-2259.
5. Tu X, Miao L, Kang Y, Xia H, Tu JW, Wang Q, Tu Q, Wang JM, Hao H. Effect of *dl*-praeruptorin A on cultured neonatal rat ventricular cardiomyocytes with hypertrophy induced by endothelin-1. Methods Find. Exp. Clin. Pharmacol, 2009; 31: 231-236.
6. Zhang Z, Liu YY, Su MQ, Liang XF, Wang WF, Zhu X. Pharmacokinetics, tissue distribution and excretion study of *dl*-praeruptorin A in rats by liquid chromatography tandem mass spectrometry. Phytomedicine, 2011; 18: 527-532.
7. Veronese L, Rautaureau J, Sadler BM, Gillotin C, Petite JP, Pillegand B, Delvaux M, Masliah C, Fosse S, Lou Y, Stein DS. Single-dose pharmacokinetics of amprenavir, a human immunodeficiency virus type 1 protease inhibitor, in subjects with normal or impaired hepatic function. Antimicrob. Agents Chemother, 2000; 44: 821-826.
8. Kang KW, Kim YG, Cho MK, Bae SK, Kim CW, Lee MG, Kim SG. Oltipraz regenerates cirrhotic liver through CCAAT/enhancer binding protein-mediated stellate cell inactivation. FASEB. J, 2002; 16: 1988-1990.
9. Jezequel AM, Mancini R, Rinaldesi ML. A morphological study of the early stages of hepatic fibrosis induced by low doses of dimethylnitrosamine in the rat. J. Hepatol, 1987; 6: 174-181.

10. Bae SK, Lee SJ, Lee JY, Lee Y, Lee I, Kim SG, Lee MG. Pharmacokinetic changes of oltipraz after intravenous and oral administration to rats with liver cirrhosis induced by dimethylnitrosamine. Int. J. Pharm, 2004; 275: 227-238.
11. Kamataki T, Kitagawa H. Effects of lyophilization and storage of rat liver microsomes on activity of aniline hydroxylase, contents of cytochrome b5 and cytochrome P-450 and aniline-induced P-450 difference spectrum. Jpn. J. Pharmacol, 1974; 24: 195-203.
12. Bradford MM. A rapid and sensitive method for the quantitation of microgram quantities of protein utilizing the principle of protein-dye binding. Anal. Biochem, 1976; 72: 248-254.
13. Ruan H, Zhang Z, Zhu X. Liquid chromatography tandem mass spectrometry pharmacokinetic study of *dl*-praeruptorin A in rat plasma. Biomed. Chromatogr, 2010; 24: 1193-1198.
14. Duggleby RG. Analysis of enzyme progress curves by nonlinear regression. Methods Enzymol, 1995; 249: 61-90.
15. Kim SH, Choi YM, Lee MG. Pharmacokinetics and pharmacodynamics of furosemide in protein-calorie malnutrition. J. Pharmacokinet. Biopharm, 1993; 21: 1-17.
16. Morgan DJ, McLean AJ. Therapeutic implications of impaired hepatic oxygen diffusion in chronic liver disease. Hepatology, 1991; 14:1280-1282.
17. Goeting NL, Fleming JS, Gallagher P, Walmsely BH, Karran SJ. Alterations in liver blood flow and reticuloendothelial function in progressive cirrhosis in the rat. J. Nucl. Med, 1986; 27: 1751-1754.
18. Ahn CY, Bae SK, Bae SH, Kim T, Jung YS, Kim YC, Lee MG, Shin WG. Pharmacokinetics of oltipraz in diabetic rats with liver cirrhosis. Brit. J. Pharmacol, 2009; 156: 1019-1028.